

Quandle Cohomology Quiver Representations

Sam Nelson*

Abstract

We define a family of quiver representation-valued invariants of oriented classical and virtual knots and links associated to a choice of finite quandle X , abelian group A , set of quandle 2-cocycles $C \subset H_Q^2(X; A)$, choice of coefficient ring k and set of quandle endomorphisms $S \subset \text{Hom}(X, X)$. From this representation we define four new polynomial (or “polynomial” depending on A) invariants. We generalize to the case of biquandles and compute some small but illustrative examples.

KEYWORDS: Quandle quivers, quandle cohomology, quiver representations, knot invariants, virtual knot invariants

2020 MSC: 57K12

1 Introduction

Quandles, an algebraic structure encoding the Reidemeister moves of knot theory analogously to the way groups encode the symmetries of geometric spaces, were introduced in [10] and independently in [13]. Quandle cohomology and quandle cocycle invariants of oriented classical and virtual knots and links, as well as quandle cocycle invariants of oriented surface-links, were introduced in [2] and further developed in [3] and other work.

Quandle coloring quivers were introduced in [6] by the author and coauthor Karina Cho. Given a finite quandle X , a subset $S \subset \text{Hom}(X, X)$ of the endomorphism set of X determines a quiver-valued invariant of oriented knots and links whose vertex set may be identified with the quandle homset $\text{Hom}(\mathcal{Q}(L), X)$ whose cardinality is the quandle counting invariant $\Phi_X^{\mathbb{Z}}(L)$. Since quivers are categories, this construction categorized the quandle counting invariant, and several new polynomial knot and link invariants were obtained in [6] via decategorification.

In [5] the quandle coloring quiver was generalized to quandle cocycle quivers to categorify the quandle 2-cocycle invariant. Since then, quivers have been used to categorify many other enhancements of homset invariants of knots, including quandle module quivers in [9], biquandle bracket quivers in [8], psyquandle coloring quivers in [4] and many more.

Many popular categorized knot and link invariants, e.g. Khovanov Homology in its various forms and extensions, start with *quiver representations*, i.e., assignments of vector spaces or modules to the vertices and linear transformations to the edges of a quiver. In this paper we introduce a quiver representation-valued invariant of oriented classical and virtual knots and links using quandle cohomology called the *quandle cohomology quiver representation* invariant. We decategorify to obtain new polynomial invariants as an application. We generalize slightly to the case of biquandles and compute some examples.

The paper is organized as follows. In Section 2 we review the basics of quandles, quandle (co)homology and quandle coloring quivers. In Section 3 we introduce the new structure of quandle cohomology quivers and compute an example to show the process. In Section 4 we generalize slightly to the case of biquandles. In Section 5 we collect some examples and computations, and we conclude in Section 6 with some questions for future research.

This paper, including all text, diagrams and computational code, was produced strictly by the author without the use of generative AI in any form.

*Email: Sam.Nelson@cmc.edu. Partially supported by Simons Foundation collaboration grant 702597.

2 Quandles, Quandle Cohomology and Quandle Coloring Quivers

We begin with a definition; see [7, 10] for more details.

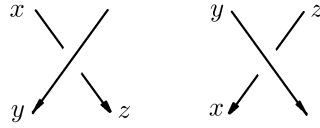
Definition 1. A *quandle* is a set X with a binary operation $\triangleright : X \times X \rightarrow X$ satisfying the axioms

- (i) For all $x \in X$ we have $x \triangleright x = x$,
- (ii) For all $y \in X$, the map $\beta_y : X \rightarrow X$ defined by $\beta_y(x) = x \triangleright y$ is invertible, and
- (iii) For all $x, y, z \in X$ we have $(x \triangleright y) \triangleright z = (x \triangleright z) \triangleright (y \triangleright z)$.

The element $\beta_y^{-1}(x)$ is often denoted $x \triangleright^{-1}y$, and indeed X is a quandle under \triangleright^{-1} known as the *dual quandle* of (X, \triangleright) . A quandle in which $\beta_y^{-1} = \beta_y$ for all $y \in X$ is called an *involutory quandle* or *kei* (圭).

Example 1. Standard examples of quandles include

- *n-fold conjugation quandles*: A group G is a quandle under $x \triangleright y = y^{-n}xy^n$ for any choice of $n \in \mathbb{Z}$,
- *Core quandles*: A group G is a quandle (indeed, a kei) under $x \triangleright y = yx^{-1}y$,
- *Alexander quandles*: A module M over the ring of Laurent polynomials $\Lambda = \mathbb{Z}[t^{\pm 1}]$ is a quandle under $\vec{x} \triangleright \vec{y} = t\vec{x} + (1-t)\vec{y}$ and
- *Knot quandles*: Given an oriented classical or virtual knot or link L represented by a diagram D , the *knot quandle* of L (also called the *fundamental quandle* of L , denoted $\mathcal{Q}(L)$) is given by a presentation with a generator for each arc in D and a relation of the form $x \triangleright y = z$ at each crossing in D as shown.



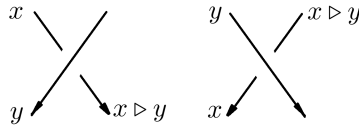
Remark 1. Joyce [10] shows that the knot quandle determines the knot group system and hence determines the knot complement up to homeomorphism. For virtual knots the knot quandle is known not to be a complete invariant [11].

Definition 2. Let X, Y be quandles. Then a map $f : X \rightarrow Y$ is a *quandle homomorphism* if for all $x, y \in X$ we have

$$f(x \triangleright y) = f(x) \triangleright f(y).$$

A quandle homomorphism $f : X \rightarrow X$ is an *endomorphism*.

Let L be an oriented classical or virtual knot or link represented by a diagram D and let X be a quandle. An assignment of an element of X to each of the arcs in D such that at every crossing we have



(with colors passing through unchanged at any virtual crossings) is called an *X-coloring* of D . Each X -coloring of D determines a unique homomorphism from the knot quandle $\mathcal{Q}(L)$ to X . In particular, the quandle axioms are chosen so that this set of quandle homomorphisms is invariant under Reidemeister moves, with the elements of the abstract homset $\text{Hom}(\mathcal{Q}(L), X)$ represented by X -colored diagrams analogously to matrices encoding linear transformations and with X -colored Reidemeister moves playing the role of change-of-basis matrices.

Example 2. Consider the $(4,2)$ -torus link $L = L4a1$ and the quandle $X = \text{Core}(\mathbb{Z}_4)$, given by the operation table (where we use the representative “4” for the class of zero so our elements match our row/column numbering):

\triangleright	1	2	3	4
1	1	3	1	3
2	4	2	4	2
3	3	1	3	1
4	2	4	2	4

The homset $\text{Hom}(\mathcal{Q}(L4a1), \text{Core}(\mathbb{Z}_4))$ is then

$$\left\{ \begin{array}{c} \text{Diagram 1} \\ \text{Diagram 2} \\ \text{Diagram 3} \\ \text{Diagram 4} \\ \text{Diagram 5} \\ \text{Diagram 6} \\ \text{Diagram 7} \\ \text{Diagram 8} \end{array} \right\}.$$

Now, let X be a finite quandle and A an abelian group. Following [2], we recall:

- The module of *rack n -chains* $C_n^R(X; A) = A[X^n]$ consists of all A -linear combinations of ordered n -tuples of elements of X ,
- The module of *degenerate n -chains* $C_n^D(X; A)$ is the submodule generated by n -tuples of the form (x_1, \dots, x_n) where $x_j = x_{j+1}$ for some j ,
- The module of *quandle n -chains* $C_n^Q(X; A) = C_n^R(X; A)/C_n^D(X; A)$ is the quotient,
- The *quandle boundary map* $\partial_n : C_n^Q(X; A) \rightarrow C_{n-1}^Q(X; A)$ is defined on generators by

$$\partial_n(x_1, \dots, x_n) = \sum_{k=1}^n (-1)^k ((x_1, \dots, x_{k-1}, x_{k+1}, \dots, x_n) - (x_1 \triangleright x_k, \dots, x_{k-1} \triangleright x_k, x_{k+1}, \dots, x_n))$$

and extended linearly (modulo degenerate chains),

- The k th *quandle homology* $H_K^Q(X; A) = \text{Ker } \partial_K^Q / \text{Im } \partial_{K+1}^Q$ is the quotient of the kernel of ∂_K modulo the image of ∂_{K+1} , and
- *Quandle cohomology* is obtained from quandle homology by dualizing in the usual way. See [2, 7] for more details.

An element of a quandle homset $\text{Hom}(\mathcal{Q}(L), X)$ determines an element $\vec{v} \in C_2^Q(X; \mathbb{Z})$ by interpreting each X -colored crossing as a signed ordered 2-tuple:

$$\begin{array}{ccc} \begin{array}{c} x \diagdown \\ y \diagup \end{array} & \begin{array}{c} y \diagdown \\ x \diagup \end{array} & \begin{array}{c} x \diagdown \\ x \diagup \end{array} \\ (x, y) & -(x, y) & 0 \end{array}.$$

Example 3. Using the ordered basis $\{(1, 2), (1, 3), (1, 4), (2, 1), (2, 3), (2, 4), (3, 1), (3, 2), (3, 4), (4, 1), (4, 2), (4, 3)\}$ for $C_2^Q(\text{Core}(\mathbb{Z}_4); \mathbb{Z})$ the homset in Example 2 determines the multiset

$$\{4 \times [0 \ 0 \ 0 \ 0 \ 0 \ 0 \ 0 \ 0 \ 0 \ 0 \ 0 \ 0]^T, 4 \times [1 \ 0 \ 0 \ 1 \ 0 \ 0 \ 0 \ 0 \ 1 \ 0 \ 0 \ 1]^T, 4 \times [0 \ 0 \ 1 \ 0 \ 1 \ 0 \ 0 \ 1 \ 0 \ 1 \ 0 \ 0]^T, \\ 2 \times [0 \ 2 \ 0 \ 0 \ 0 \ 0 \ 2 \ 0 \ 0 \ 0 \ 0 \ 0]^T, 2 \times [0 \ 0 \ 0 \ 0 \ 0 \ 2 \ 0 \ 0 \ 0 \ 0 \ 2 \ 0]^T\}.$$

We can evaluate $\phi \in C_Q^2(X; A)$ on a vector $\vec{v} \in C_2^Q(X; \mathbb{Z})$ to obtain an element $\langle \phi, \vec{v} \rangle \in A$ since A is a \mathbb{Z} -module, i.e., for $a \in A$ and $n \in \mathbb{Z}$ we have

$$an = \begin{cases} \overbrace{a + a + \cdots + a}^n & n > 0 \\ 0 & n = 0 \\ \underbrace{-a - a - \cdots - a}_{-n} & n < 0 \end{cases}.$$

The quandle boundary map is chosen so that evaluating a cocycle $\phi \in C_Q^2(X; A)$ on a vector $\vec{v} \in C_2^Q(X; \mathbb{Z})$ arising from a quandle homset element yields a scalar $\phi(\vec{v}) \in A$ called a *Boltzmann weight* which is unchanged by X -colored Reidemeister moves. More precisely, we have the following standard result (see [2]) which we include for completeness:

Theorem 1. (*Carter, Jelovsky, Kamada, Langford and Saito*) *If $\vec{v}, \vec{v}' \in C_2^Q(X; \mathbb{Z})$ represent X -colored diagrams differing by a Reidemeister move and $\phi \in C_Q^2(X; A)$, then $\langle \phi, \vec{v} \rangle = \langle \phi, \vec{v}' \rangle$.*

Proof. Checking each of the Reidemeister moves, we see that the Boltzmann weight contribution is the same on both sides of the move. Here we will show one oriented case of each of the three Reidemeister moves; the reader is invited to verify the others.

$\phi(x, x) = 0$
 $\phi(x, y) - \phi(x, y) = 0$

$\phi(x, y) + \phi(y, z) + \phi(x \triangleright y, z) = \phi(x, z) + \phi(y, z) + \phi(x \triangleright z, y \triangleright z)$
 $\iff \phi(y, z) - \phi(y, z) - \phi(x, z) + \phi(x \triangleright y, z) + \phi(x, y) - \phi(x \triangleright z, y \triangleright z) = 0$

which is satisfied since $\phi \in H_Q^2(X; A)$. □

It follows that the multiset M of Boltzmann weights for a choice of quandle 2-cocycle $\phi \in C_Q^2(X; A)$ is an invariant of oriented knots and links. For ease of comparison, it is standard to convert the multiset M into a “polynomial” form

$$\Phi_\phi(q) = \sum_{m \in M} q^m$$

generally known as the *quandle 2-cocycle polynomial*. Evaluating $q = 1$ then yields the quandle counting invariant $|\text{Hom}(\mathcal{Q}(L), X)|$. See [2, 7] for more.

Remark 2. When $A = \mathbb{Z}$, Φ_ϕ is a Laurent polynomial, while for other coefficient groups since the exponents are elements of A , the polynomial form should not be taken too literally as a polynomial but regarded as a convenient bookkeeping device for representing the multiset. For those distressed by this notation, we could instead use a complex or matrix representation for A , e.g., write $A = \mathbb{Z}_n$ multiplicatively as the n th roots of unity; alternatively, we could polynomialize M by taking $\Phi'_\phi(q) = \prod_{m \in M} (q - m) \in \mathbb{Z}[A, q]$ to obtain a polynomial with $\mathbb{Z}[A]$ coefficients whose roots are the elements of M and whose degree recovers the counting invariant.

Example 4. In the dual of the basis from Example 3, $H_Q^2(\text{Core}(\mathbb{Z}_4); \mathbb{Z})$ has basis

$$\{[1 \ 0 \ 1 \ 0 \ 0 \ 0 \ 0 \ 0 \ 0 \ 0], [0 \ 0 \ 0 \ 0 \ 0 \ 0 \ 1 \ 1 \ 0 \ 0]\}.$$

Applying the first cocycle to the homset in Example 3 yields quandle 2-cocycle invariant

$$M = \{8 \times 0, 8 \times 1\}$$

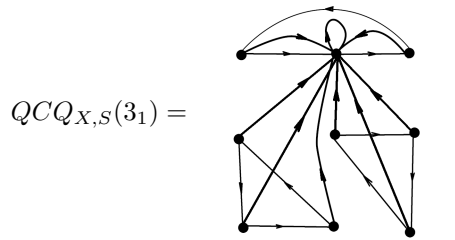
or in polynomial form, $8 + 8q$.

Let X be a finite quandle and $\sigma \in \text{Hom}(X, X)$ a quandle endomorphism. As observed in [6], applying σ to the colors on an X -colored oriented classical or virtual knot or link diagram results in another X -colored diagram:

$$\begin{array}{ccc} \begin{array}{c} x \searrow \\ y \swarrow \end{array} & \xrightarrow{\sigma} & \begin{array}{c} \sigma(x) \searrow \\ \sigma(y) \swarrow \end{array} \\ & & \sigma(x \triangleright y) = \sigma(x) \triangleright \sigma(y) \end{array}$$

It then follows that assigning a vertex to each X -coloring in the quandle homset, each endomorphism determines a directed edge from each vertex to some other (possibly the same) vertex, resulting in a *quiver* or directed graph called the *quandle coloring quiver* associated to the knot or link L , denoted $QCQ_{X,S}(L)$. If $S = \text{Hom}(X, X)$ we say $QCQ_{X,S}(L)$ is the *full quiver*.

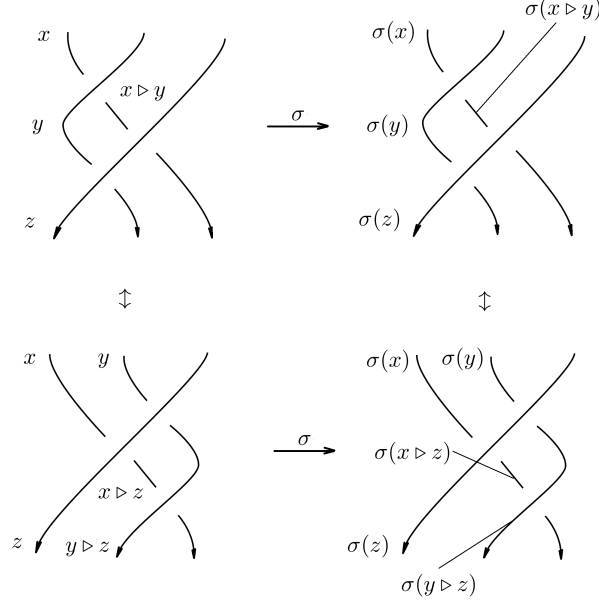
Example 5. Let $X = \text{Core}(\mathbb{Z}_3)$. Then writing endomorphisms $\sigma : X \rightarrow X$ as vectors of images of elements of X , i.e., $\sigma = [\sigma(1), \sigma(2), \sigma(3)]$, choosing the set $S = \{[1, 1, 1], [2, 3, 1]\} \subset \text{Hom}(X, X)$ we obtain quandle coloring quiver for the trefoil knot



Theorem 2. (Cho., N. [6]) *The quandle coloring quiver determined by a choice of quandle X and set $S \subseteq \text{Hom}(X, X)$ of endomorphisms is an invariant of oriented classical and virtual knots and links.*

Proof. This follows immediately from the fact that each σ is an endomorphism of X ; changing the diagram by Reidemeister moves carries the quandle coloring along in a bijective way, and applying the same endomorphism σ to a diagram before or after a move commutes with the move. For example, let us illustrate the

case of the commutative square of a Reidemeister III move:



The other moves are similar; see [6] for more details. \square

3 Quandle Cohomology Quivers and Representations

In this section we introduce a new invariant of oriented classical knots and links in the form of a quiver representation and use it to obtain new enhancements of the quandle counting invariant.

Definition 3. Let X be a finite quandle and A an abelian group. Each endomorphism $\sigma \in \text{Hom}(X, X)$ induces a linear transformation $\sigma : C_2^Q(X; \mathbb{Z}) \rightarrow C_2^Q(X; \mathbb{Z})$ by setting

$$\sigma \left(\sum \alpha(x_j, x_k) \right) = \sum \alpha(\sigma(x_j), \sigma(x_k)).$$

Next we define the key elements of our quiver representation.

Definition 4. Let X be a finite quandle, A an abelian group, C a finite subset of $H_Q^2(X; A)$, k a coefficient ring and S a subset of the endomorphism set $\text{Hom}(X, X)$. Let K be an oriented classical or virtual knot or link represented by a diagram D . Then for each X -coloring of D in $\text{Hom}(Q(D), X)$, the associated vector $\vec{v} \in C_2^Q(X; \mathbb{Z})$ pairs with each element $\phi \in C$ to yield an element $\phi(\vec{v}) \in A$. We then define $V_C(\vec{v})$ to be the subspace of $k[A]$ generated by $\{\phi(\vec{v}) \mid \phi \in C\} \subset A$. Moreover, for each $\phi \in C$, we define a linear transformation $f_\sigma : k[A] \rightarrow k[A]$ by first setting for each $\phi \in C$

$$f_{\sigma, \phi}(\phi(\vec{v})) = \phi(\sigma(\vec{v}))$$

and extending linearly, then setting

$$f_\sigma = \sum_{\phi \in C} f_{\sigma, \phi}.$$

That is, each vertex gets a copy of $k[A]$ with a distinguished subspace $V_C(\vec{v})$ determined by the cocycle values on the coloring vector at the vertex; then each endomorphism $\sigma \in S$ determines a linear transformation $f_\sigma : k[A] \rightarrow k[A]$ sending distinguished subspaces to distinguished subspaces.

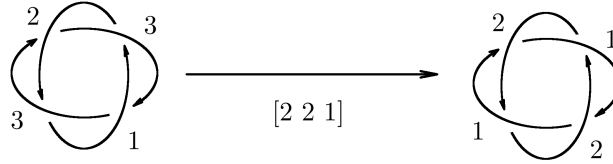
Example 6. Let $k = \mathbb{Z}$ and $A = \mathbb{Z}_3 = \{0, 1, 2\}$ (which we might write as $\{\vec{0}, \vec{1}, \vec{2}\}$ when we think of the elements of A as generating vectors for $k[A]$). Let X be the quandle defined by the operation table

\triangleright	1	2	3
1	1	1	2
2	2	2	1
3	3	3	3

then $H_Q^2(X; \mathbb{Z}_3)$ is generated by the vectors

$$C = \{[0 \ 1 \ 0 \ 1 \ 0 \ 0], [0 \ 0 \ 1 \ 0 \ 0 \ 0], [0 \ 0 \ 0 \ 0 \ 0 \ 1]\}$$

written in the basis $\{(1, 2), (1, 3), (2, 1), (2, 3), (3, 1), (3, 2)\}$ for $C_Q^2(X; \mathbb{Z}_3)$. The quandle coloring quiver for the link $L4a1$ with endomorphism $\sigma = [2 \ 2 \ 1]$ includes the arrow



from the X -coloring given by coloring vector $\vec{v} = [0 \ 1 \ 0 \ 1 \ 1 \ 1]^T$ to the X -coloring given by coloring vector $\sigma(\vec{v}) = [2 \ 0 \ 2 \ 0 \ 0 \ 0]^T$. Then applying the cocycles in C to these coloring vectors yields linear maps

$$[0 \ 1 \ 0 \ 1 \ 0 \ 0] \begin{bmatrix} 0 \\ 1 \\ 0 \\ 1 \\ 1 \\ 1 \end{bmatrix} \xrightarrow{\sigma} [0 \ 1 \ 0 \ 1 \ 0 \ 0] \begin{bmatrix} 2 \\ 0 \\ 2 \\ 0 \\ 0 \\ 0 \end{bmatrix} \Rightarrow \vec{2} \mapsto \vec{0} \Rightarrow \begin{bmatrix} 0 & 0 & 1 \\ 0 & 0 & 0 \\ 0 & 0 & 0 \end{bmatrix},$$

$$[0 \ 0 \ 1 \ 0 \ 0 \ 0] \begin{bmatrix} 0 \\ 1 \\ 0 \\ 1 \\ 1 \\ 1 \end{bmatrix} \xrightarrow{\sigma} [0 \ 0 \ 1 \ 0 \ 0 \ 0] \begin{bmatrix} 2 \\ 0 \\ 2 \\ 0 \\ 0 \\ 0 \end{bmatrix} \Rightarrow \vec{0} \mapsto \vec{2} \Rightarrow \begin{bmatrix} 0 & 0 & 0 \\ 0 & 0 & 0 \\ 1 & 0 & 0 \end{bmatrix}$$

and

$$[0 \ 0 \ 0 \ 0 \ 0 \ 1] \begin{bmatrix} 0 \\ 1 \\ 0 \\ 1 \\ 1 \\ 1 \end{bmatrix} \xrightarrow{\sigma} [0 \ 0 \ 0 \ 0 \ 0 \ 1] \begin{bmatrix} 2 \\ 0 \\ 2 \\ 0 \\ 0 \\ 0 \end{bmatrix} \Rightarrow \vec{1} \mapsto \vec{0} \Rightarrow \begin{bmatrix} 0 & 1 & 0 \\ 0 & 0 & 0 \\ 0 & 0 & 0 \end{bmatrix}.$$

Thus we have $V_C(\vec{v}) = \mathbb{Z}[\vec{0}, \vec{1}, \vec{2}] = \mathbb{Z}[\mathbb{Z}_3]$, $V_C(\sigma(\vec{v})) = \mathbb{Z}[\vec{0}, \vec{2}] \subset \mathbb{Z}[\mathbb{Z}_3]$ and $f_\sigma : \mathbb{Z}[\mathbb{Z}_3] \rightarrow \mathbb{Z}[\mathbb{Z}_3]$ defined by the matrix

$$f_\sigma = \begin{bmatrix} 0 & 1 & 1 \\ 0 & 0 & 0 \\ 1 & 0 & 0 \end{bmatrix}.$$

We can now make our main new definition and state our main proposition.

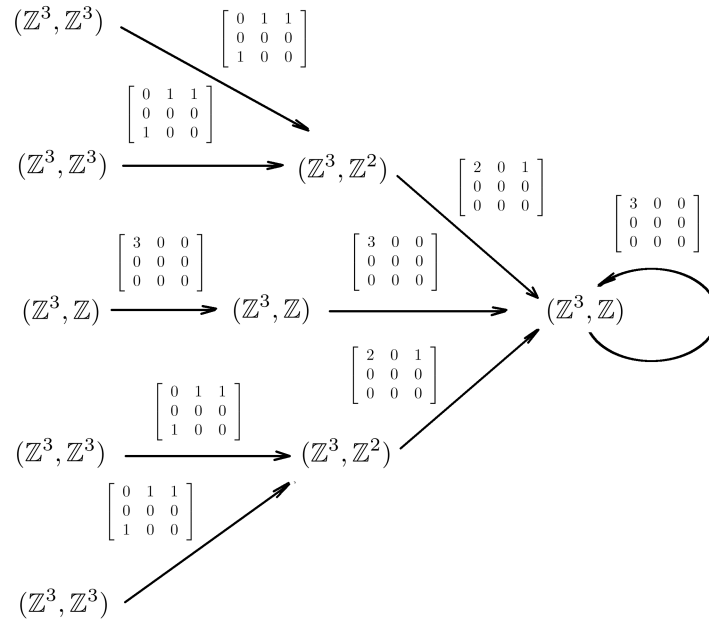
Definition 5. Let X be a finite quandle, A an abelian group, $C \subset H_Q^2(X; A)$ a finite set of quandle 2-cocycles representing quandle cohomology classes, L an oriented classical or virtual knot or link represented by a diagram D , k a coefficient ring and $S \subset \text{Hom}(X, X)$ a set of quandle endomorphisms. We will refer to the 5-tuple (X, A, C, k, S) as the *quandle cohomology quiver representation data vector* or just the *data vector*. Then we define the *quandle cohomology quiver representation* of K to be the quandle coloring quiver of K with respect to (X, S) with each vertex \vec{v} weighted with the pair $(k[A], V_C(\vec{v}))$ and each edge defined by $\sigma \in S$ weighted with f_σ .

Then we have:

Proposition 3. *The quandle cohomology quiver representation of K is unchanged by Reidemeister moves on D and hence is an invariant of oriented classical and virtual knots and links.*

Proof. Reidemeister moves on D induce isomorphisms on the quandle coloring quiver and do not change the cocycle values $\langle \phi, \vec{v} \rangle$. It then follows that vector spaces $(k[A], V_C(\vec{v}))$ and edge maps f_σ are also preserved by the quiver isomorphism. \square

Example 7. Computing the rest of the quiver representation for the link in Example 6, we get



Quiver representations form the starting point for many knot and link invariants such as Khovanov homology as well as many other structures of interest. We anticipate exploring many such avenues in future work. For the present, we will content ourselves with the following new families of invariants.

When defining new knot invariants, it is often necessary to strike a compromise between strength and ease of use. One reasonable choice for a polynomial invariant of matrices is the characteristic polynomial $\chi(M) = \det(tI - M)$; while not completely determining M , it nonetheless retains most of the information about the linear transformation and is generally much more compact and easy to compare. Another convenient choice is to encode a square matrix M as a *matrix polynomial*

$$p_M(x, y) = \sum_{j, k \in A} M_{j, k} x^j y^k$$

where A is a set of labels for the rows and columns of M . This polynomial actually determines the matrix, given the row/column labels:

$$\begin{bmatrix} 1 & 0 & 2 \\ 3 & 0 & 0 \\ 0 & 0 & 2 \end{bmatrix} \leftrightarrow 1x^0y^0 + 2x^0y^2 + 3x^1y^0 + 2x^2y^2$$

assuming a label set of $A = \{0, 1, 2\}$. We caution that depending on the choice of A , we should regard this “polynomial” as a bookkeeping device and not take it too literally as a polynomial since the exponents are elements of A .

With these in mind, let us now define our new polynomial invariants.

Definition 6. Let Q be a quandle cocycle quiver representation with data vector (X, A, C, k, S) . We define the *quandle cohomology quiver representation edge characteristic polynomial* or just the *edge characteristic polynomial* to be the sum

$$\Phi_\chi^E(t) = \sum_{e \in Q} \chi(f_\sigma)$$

of the characteristic polynomials of the matrices f_σ associated to each edge. We further define the *quandle cohomology quiver representation edge matrix polynomial* or just the *edge matrix polynomial* to be the sum

$$\Phi_{p_M}^E(x, y) = \sum_{e \in Q} p_M(f_\sigma)$$

of the matrix polynomials encoding the matrices representing f_σ on each edge.

Example 8. The quiver representation in Example 7 has edge characteristic polynomial $\Phi_\chi^E(t) = 9t^3 - 13t^2 - 4t$ and edge 2-variable polynomial $\Phi_{p_M}^E(x, y) = 4x^2 + 6y^2 + 4y + 13$.

These two polynomials include information about all of the matrices associated to the edges in Q , but they don’t make explicit use of the overall quiver structure of Q . For this, let us consider the set of paths in our quiver which are:

- maximal in the sense of not being a subpath of any other path, and
- non-repeating, i.e. not repeating any edge.

Remark 3. We note that since every vertex has out-degree $|S|$, maximal paths may start at a leaf but cannot end at one. Generically, a maximal non-repeating path starts at a leaf or cycle and connects to other cycles.

Definition 7. Let Q be a quandle cocycle quiver representation. For each maximal directed path $P_j = e_1e_2 \dots e_k$ in Q without repeated edges, in the corresponding sequence of vector spaces and maps

$$V_1 \xrightarrow{f_1} V_2 \xrightarrow{f_2} \dots \xrightarrow{f_k} V_{k+1},$$

let $M_j = f_k \dots f_2f_1$ be the the matrix product. Then we define the *quandle cohomology quiver representation maximal path characteristic polynomial* or just the *path characteristic polynomial* to be the sum

$$\Phi_\chi^P = \sum_j \chi(M_j) s^{|j|}$$

of characteristic polynomials of M_j times a variable s to the power of the length of the path j over the set of maximal nonrepeating paths in Q , and we define the *quandle cohomology quiver representation maximal path matrix polynomial* or just the *path matrix polynomial* to be the sum

$$\Phi_{p_M}^P(x, y) = \sum_j p_M(M_j) z^{|j|}$$

of products of p_M values of M_j times z to the power of the length of the paths j over the set of maximal nonrepeating paths in Q .

We then have:

Proposition 4. *The polynomials Φ_χ^E , Φ_χ^P , $\Phi_{p_M}^E$ and $\Phi_{p_M}^P$ are invariants of classical and virtual oriented knots and links for every choice of finite quandle X , abelian group A , set of quandle cocycles $C \subset H_Q^2(x; A)$, coefficient ring k and set of quandle endomorphisms $S \subset \text{Hom}(X, X)$.*

Proof. Changing the diagram by a Reidemeister move induces a quiver isomorphism preserving the vector spaces $(k[A], V_C(\vec{v}))$ and the matrices f_σ . Hence, Φ_χ^E , Φ_χ^P , $\Phi_{p_M}^E$ and $\Phi_{p_M}^P$ are unchanged by Reidemeister moves and thus are knot invariants. \square

Example 9. In the quiver representation in Example 7, there are five maximal paths without repeating edges, each starting from a leaf and ending at the loop. Then four of the edges have matrix product

$$\begin{bmatrix} 3 & 0 & 0 \\ 0 & 0 & 0 \\ 0 & 0 & 0 \end{bmatrix} \begin{bmatrix} 2 & 0 & 1 \\ 0 & 0 & 0 \\ 0 & 0 & 0 \end{bmatrix} \begin{bmatrix} 0 & 1 & 1 \\ 0 & 0 & 0 \\ 1 & 0 & 0 \end{bmatrix} = \begin{bmatrix} 3 & 0 & 0 \\ 0 & 0 & 0 \\ 0 & 0 & 0 \end{bmatrix} \begin{bmatrix} 1 & 2 & 2 \\ 0 & 0 & 0 \\ 0 & 0 & 0 \end{bmatrix} = \begin{bmatrix} 3 & 6 & 6 \\ 0 & 0 & 0 \\ 0 & 0 & 0 \end{bmatrix}$$

and the other has matrix

$$\begin{bmatrix} 3 & 0 & 0 \\ 0 & 0 & 0 \\ 0 & 0 & 0 \end{bmatrix}^3 = \begin{bmatrix} 27 & 0 & 0 \\ 0 & 0 & 0 \\ 0 & 0 & 0 \end{bmatrix}.$$

All maximal non-repeating paths in this quiver have length 3. Then the path characteristic polynomial is $\Phi_\chi^P(t) = 5s^3t^3 - 39s^3t^2$ and the path matrix polynomial is $\Phi_{p_M}^P(x, y) = 24x^2z^3 + 24xz^3 + 39z^3$.

Example 10. If the set S consists only of the identity endomorphism and the set C of cocycles consists of a single cocycle ϕ , then each path matrix has a single 1 in the row and column corresponding to the basis element $\phi(\vec{v})$ of $k[A]$. Then the path matrix polynomial equals the edge polynomial after evaluating at $z = 1$ and setting $xy = q$ yields the original quandle 2-cocycle invariant; hence, this family of invariants includes the quandle 2-cocycle invariants as a special case. If we further choose the cocycle to be a coboundary and $k = \mathbb{Z}$, then (interpreting $(xy)^0 = 1$) the polynomial is an integer, more precisely the number of quandle colorings of L , i.e., the quandle counting invariant. We further note that if C includes several quandle cocycles and $S = \{\text{Id}_X\}$ then the common value of the edge and path polynomials with $z = 1$ is a kind of “multi-2-cocycle” invariant similar to the invariant described in [12].

4 Generalization to Biquandles

In this section we generalize the construction from the previous section to the case of biquandles. This has the advantage of giving us more invariants with smaller operation tables for quicker computation as well as stronger invariants for the case of virtual knots and links. See [7] for more details.

Definition 8. A *biquandle* is a set X with two binary operations $\rhd, \bar{\rhd} : X \times X \rightarrow X$ satisfying the axioms

- (i) For all $x \in X$, $x \rhd x = x \bar{\rhd} x$,
- (ii) For all $y \in X$ the maps $\alpha_y, \beta_y : X \rightarrow X$ and the map $S : X \times X \rightarrow X \times X$ defined by $\alpha_y(x) = x \bar{\rhd} y$, $\beta_y(x) = x \rhd y$ and $S(x, y) = (y \bar{\rhd} x, x \rhd y)$ are invertible and
- (iii) For all $x, y, z \in X$ we have the *exchange laws*

$$\begin{aligned} (x \rhd y) \rhd (z \rhd y) &= (x \rhd z) \rhd (y \bar{\rhd} z) \\ (x \rhd y) \bar{\rhd} (z \rhd y) &= (x \bar{\rhd} z) \rhd (y \bar{\rhd} z) \\ (x \bar{\rhd} y) \bar{\rhd} (z \bar{\rhd} y) &= (x \bar{\rhd} z) \bar{\rhd} (y \rhd z). \end{aligned}$$

Example 11. Standard examples of biquandles include

- *Quandles* are biquandles with $x \bar{\triangleright} y = x$ for all $x, y \in X$,
- *Alexander biquandles* are modules over $\mathbb{Z}[t^{\pm 1}, s^{\pm 1}]$ with $x \triangleright y = tx + (s - t)y$ and $x \bar{\triangleright} y = sx$,
- Groups are biquandles under the operations $x \triangleright y = y^{-1}xy^{-1}$ and $x \bar{\triangleright} y = x^{-1}$ and
- Oriented classical and virtual knots and links have an associated *fundamental biquandle* or *knot biquandle* defined via a presentation from any diagram of the knot or link. See [7] for more.

Definition 9. A map $f : X \rightarrow Y$ between biquandles such that for all $x, y \in X$ we have

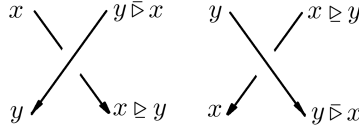
$$f(x \triangleright y) = f(x) \triangleright f(y) \quad \text{and} \quad f(x \bar{\triangleright} y) = f(x) \bar{\triangleright} f(y)$$

is a *biquandle homomorphism*; a biquandle homomorphism $\sigma : X \rightarrow X$ is a *biquandle endomorphism*.

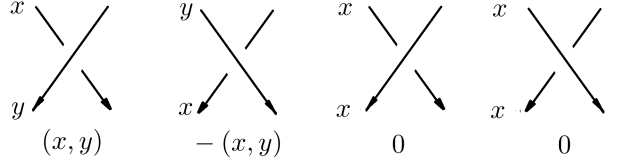
Biquandle (co)homology is defined analogously to quandle (co)homology with the biquandle boundary map given by

$$\partial_n(x_1, \dots, x_n) = \sum_{k=1}^n (-1)^k ((x_1, \dots, x_{k-1}, x_{k+1}, \dots, x_n) - (x_1 \triangleright x_k, \dots, x_{k-1} \triangleright x_k, x_{k+1} \bar{\triangleright} x_k, \dots, x_n \bar{\triangleright} x_k)).$$

The coloring rule for biquandle colorings of oriented link diagrams is (ignoring virtual crossings)



where we color *semiarcs* divided at both over- and under-crossings, and translating X -colored diagrams to 2-chains uses



Example 12. The smallest nontrivial biquandle is $\mathbb{Z}_2 = \{1, 2\}$ (writing the class of zero as 2 so our entries match our row/column numbers) with operations $x \triangleright y = x \bar{\triangleright} y = x + 1$. Then both ∂_3 and ∂_2 are zero, so $H_Q^2(X; A)$ is generated by $\{[1 \ 0], [0 \ 1]\}$ when written in the ordered basis $\{(1, 2), (2, 1)\}$ for $C_Q^2(X; A)$.

The quandle cocycle quiver representation and its various polynomial decategorifications from Section 3 extend to the biquandle case by replacing quandles and quandle homomorphisms with biquandles and biquandle homomorphisms; indeed, the former is a special case of the latter.

Remark 4. It was shown in [10] that the knot quandle is a complete invariant of classical knots up to ambient homeomorphism, and the knot biquandle is easily seen to be unchanged by reversed orientation mirror image; it follows that for classical knots, the knot quandle already contains the same information as the knot biquandle. However, for virtual knots and links, the knot biquandle is known to be stronger than the knot quandle, and in any case the same information presented in different forms can have different levels of accessibility – it may be more computationally efficient to use quandles in some cases and biquandles in others, even for classical knots and links.

5 Examples and Computations

In this Section we collect some examples and computations.

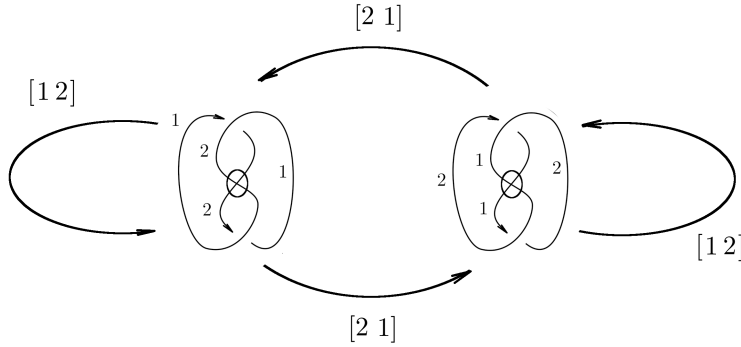
Example 13. The link in $L4a1$ with respect to the data vector consisting of quandle $X = \text{Core}(\mathbb{Z}_4)$, abelian group $A = \mathbb{Z}_3$, cocycles

$$\{[1\ 0\ 1\ 0\ 0\ 0\ 0\ 0\ 0\ 0\ 0], [0\ 0\ 0\ 0\ 0\ 0\ 0\ 1\ 1\ 0\ 0\ 0]\}$$

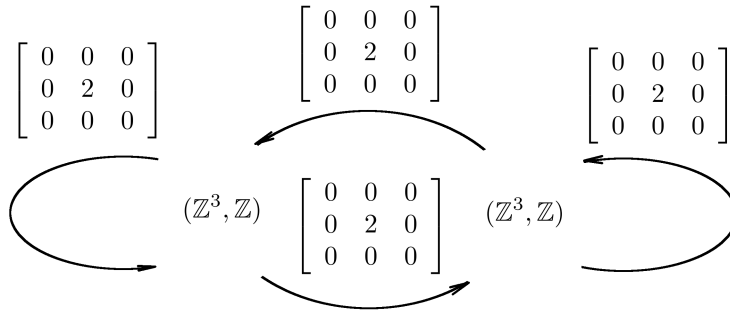
in $H_Q^2(X; \mathbb{Z}_3)$, coefficient ring $k = \mathbb{Z}$ and endomorphism set $S = \{[2, 4, 2, 4], [1, 1, 1, 1]\}$ has (via `python` computation) edge and path characteristic and matrix polynomials

$$\begin{aligned} \Phi_\chi^E &= 32t^3 - 30t^2 \\ \Phi_\chi^E &= 3y + 32 \\ \Phi_{PM}^P &= 60s^7t^3 - 1536s^7t^2 + 22s^6t^3 - 384s^6t^2 + 16s^5t^3 + 22s^4t^3 - 96s^4t^2 \cdot \\ \Phi_\chi^P &= 6144xz^7 + 1024xz^6 + 512xz^5 + 256xz^4 + 1536z^7 + 384z^6 + 96z^4 \end{aligned}$$

Example 14. Let $X = \mathbb{Z}_2$ with $x \triangleright y = x \bar{\triangleright} y = x + 1$, $A = \mathbb{Z}_3$, $C = \{[1\ 0], [0\ 1]\} \subset H_Q^2(X; A)$ with respect to the ordered basis $\{(1, 2), (2, 1)\}$, $k = \mathbb{Z}$ and $S = \text{Hom}(X, X) = \{[1, 2], [2, 1]\}$. Then the virtual knot 2.1 has (like all classical and virtual knots) two X -colorings, both represented by the biquandle 2-chain $\{[1\ 1]^T\}$ resulting in biquandle coloring quiver



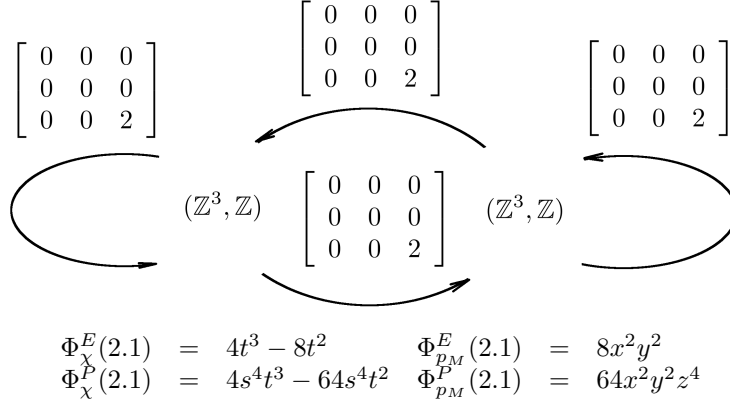
with distinguished subspace $\mathbb{Z}[\vec{1}] \subset \mathbb{Z}^3$ at each vertex and quiver representation



All maximal non-repeating paths in this quiver have length 4. We then have invariant values

$$\begin{aligned} \Phi_\chi^E(2.1) &= 4t^3 - 8t^2 & \Phi_{PM}^E(2.1) &= 8xy \\ \Phi_\chi^P(2.1) &= 4s^4t^3 - 64s^4t^2 & \Phi_{PM}^P(2.1) &= 64xyz^4 \cdot \end{aligned}$$

The mirror image of 2.1 has quiver representation



showing that these invariants are sensitive to (horizontal) mirror image.

Example 15. Using `python` code, we compute the following values for the edge characteristic and matrix polynomials for the virtual knots with up to 4 classical crossings with a choice of orientation in the table at [1] using the (X, A, C, k, S) data vector from Example 14.

$\Phi_{p_M}^E(L)$	L
$64z^4$	3.1, 3.5, 3.6, 3.7, 4.2, 4.6, 4.8, 4.10, 4.12, 4.13, 4.16, 4.17, 4.19, 4.21, 4.23, 4.24, 4.26, 4.31, 4.32, 4.35, 4.36, 4.41, 4.42, 4.46, 4.47, 4.50, 4.51, 4.55, 4.56, 4.57, 4.58, 4.59, 4.65, 4.66, 4.67, 4.68, 4.70, 4.71, 4.72, 4.75, 4.76, 4.77, 4.79, 4.85, 4.86, 4.89, 4.90, 4.93, 4.96, 4.97, 4.98, 4.99, 4.102, 4.103, 4.105, 4.106, 4.107, 4.108
$64xyz^4$	2.1, 4.1, 4.3, 4.7, 4.25, 4.28, 4.43, 4.53, 4.73, 4.80, 4.84, 4.88, 4.91, 4.100, 4.104
$64x^2y^2z^4$	3.2, 3.3, 3.4, 4.4, 4.5, 4.9, 4.11, 4.14, 4.15, 4.18, 4.20, 4.22, 4.27, 4.29, 4.30, 4.33, 4.34, 4.37, 4.38, 4.39, 4.40, 4.44, 4.45, 4.48, 4.49, 4.52, 4.54, 4.60, 4.61, 4.62, 4.63, 4.64, 4.69, 4.74, 4.78, 4.81, 4.82, 4.83, 4.87, 4.92, 4.94, 4.95, 4.101

Example 16. Computing all four polynomials for a choice of orientation for the prime classical links with up to 7 crossings as found in [1] with the choice of (X, A, C, k, S) data vector from Examples 6-7 using `python` code, we obtain the tables

L	Φ_{χ}^E	$\Phi_{p_M}^E$
$L2a1$	$5t^3 - 13t^2$	$2y + 13$
$L4a1$	$9t^3 - 13t^2 - 4t$	$4x^2 + 6y^2 + 4y + 13$
$L5a1$	$9t^3 - 24t^2$	$2y^2 + y + 24$
$L6a1$	$9t^3 - 15t^2 - 2t$	$2x^2y^2 + 2x^2 + 6y^2 + 4y + 13$
$L6a2$	$5t^3 - 15t^2$	15
$L6a3$	$5t^3 - 15t^2$	15
$L6a4$	$27t^3 - 69t^2$	$6y^2 + 6y + 69$
$L6a5$	$15t^3 - 21t^2 - 6t$	$6x^2 + 12y^2 + 6y + 21$
$L6n1$	$15t^3 - 24t^2 - 9t$	$6x^2 + 15y^2 + 24$
$L7a1$	$9t^3 - 24t^2$	$y^2 + 2y + 24$
$L7a2$	$9t^3 - 13t^2 - 2t$	$2x^2y + 2x^2 + 6y^2 + 4y + 13$
$L7a3$	$9t^3 - 23t^2$	$2y^2 + 2y + 23$
$L7a4$	$9t^3 - 23t^2$	$2y^2 + 2y + 23$
$L7a5$	$5t^3 - 13t^2$	$2y + 13$
$L7a6$	$5t^3 - 13t^2$	$2y + 13$
$L7a7$	$15t^3 - 34t^2 - 2t$	$2x^2 + 6y^2 + 3y + 34$
$L7n1$	$9t^3 - 15t^2 - 3t$	$xy^2 + xy + 2x + 2y^2 + 7y + 14$
$L7n2$	$9t^3 - 25t^2$	$2y + 25$

and

L	Φ_{χ}^P	Φ_{PM}^P
$L2a1$	$s^3t^3 - 27s^3t^2 + 2s^2t^3 - 12s^2t^2$	$6xz^2 + 27z^3 + 12z^2$
$L4a1$	$5s^3t^3 - 39s^3t^2$	$24x^2z^3 + 24xz^3 + 39z^3$
$L5a1$	$5s^3t^3 - 108s^3t^2$	$18x^2z^3 + 9xz^3 + 108z^3$
$L6a1$	$5s^3t^3 - 33s^3t^2$	$30x^2z^3 + 24xz^3 + 33z^3$
$L6a2$	$s^3t^3 - 27s^3t^2 + 2s^2t^3 - 18s^2t^2$	$27z^3 + 18z^2$
$L6a3$	$s^3t^3 - 27s^3t^2 + 2s^2t^3 - 18s^2t^2$	$27z^3 + 18z^2$
$L6a4$	$19s^3t^3 - 405s^3t^2$	$54x^2z^3 + 54xz^3 + 405z^3$
$L6a5$	$7s^3t^3 - 45s^3t^2 + 3s^2t^3 - 18s^2t^2$	$36x^2z^3 + 9x^2z^2 + 36xz^3 + 45z^3 + 18z^2$
$L6n1$	$7s^3t^3 - 63s^3t^2 + 3s^2t^3 - 18s^2t^2$	$54x^2z^3 + 9x^2z^2 + 63z^3 + 18z^2$
$L7a1$	$5s^3t^3 - 108s^3t^2$	$9x^2z^3 + 18xz^3 + 108z^3$
$L7a2$	$5s^3t^3 - 33s^3t^2$	$24x^2z^3 + 30xz^3 + 33z^3$
$L7a3$	$5s^3t^3 - 99s^3t^2$	$18x^2z^3 + 18xz^3 + 99z^3$
$L7a4$	$5s^3t^3 - 99s^3t^2$	$18x^2z^3 + 18xz^3 + 99z^3$
$L7a5$	$s^3t^3 - 27s^3t^2 + 2s^2t^3 - 12s^2t^2$	$6xz^2 + 27z^3 + 12z^2$
$L7a6$	$s^3t^3 - 27s^3t^2 + 2s^2t^3 - 12s^2t^2$	$6xz^2 + 27z^3 + 12z^2$
$L7a7$	$7s^3t^3 - 114s^3t^2 + 3s^2t^3 - 24s^2t^2$	$30x^2z^3 + 3x^2z^2 + 21xz^3 + 114z^3 + 24z^2$
$L7n1$	$5s^3t^3 - 39s^3t^2$	$15x^2z^3 + 33xz^3 + 39z^3$
$L7n2$	$5s^3t^3 - 117s^3t^2$	$18xz^3 + 117z^3$

6 Questions

We end with some questions and directions for future research.

In defining knot invariants, there is often a tradeoff between strength and usability. We have attempted to strike a good balance by passing from matrices to characteristic polynomials which retain much of the structure of the matrices while being easier to write and visually compare and with matrix “polynomials” which actually encode the matrix using row and column labels as exponents. What other decategorifications are possible? What are the geometric meanings of these invariants?

More generally, what kinds of new invariant structures can be built on this foundation? Homology theories, functorial invariants, exact sequences?

We anticipate many future projects building on this and similar definitions, including quiver representations for other homset structures, different constructions of quiver representations and further invariants to be derived from them.

References

- [1] D. Bar-Natan. The knot atlas http://katlas.org/wiki/Main_Page.
- [2] J. S. Carter, D. Jelsovsky, S. Kamada, L. Langford, and M. Saito. State-sum invariants of knotted curves and surfaces from quandle cohomology. *Electron. Res. Announc. Amer. Math. Soc.*, 5:146–156 (electronic), 1999.
- [3] J. S. Carter, S. Kamada, and M. Saito. Diagrammatic computations for quandles and cocycle knot invariants. In *Diagrammatic morphisms and applications (San Francisco, CA, 2000)*, volume 318 of *Contemp. Math.*, pages 51–74. Amer. Math. Soc., Providence, RI, 2003.
- [4] J. Cenicerros, A. Christiana, and S. Nelson. Psyquandle coloring quivers. *arXiv:2107.05668*, 2021.
- [5] K. Cho and S. Nelson. Quandle cocycle quivers. *Topology Appl.*, 268:106908, 10, 2019.

- [6] K. Cho and S. Nelson. Quandle coloring quivers. *Journal of Knot Theory and Its Ramifications*, 28(01):1950001, 2019.
- [7] M. Elhamdadi and S. Nelson. *Quandles—an introduction to the algebra of knots*, volume 74 of *Student Mathematical Library*. American Mathematical Society, Providence, RI, 2015.
- [8] P. C. Falkenburg and S. Nelson. Biquandle bracket quivers. *J. Knot Theory Ramifications (to appear)*, 2023.
- [9] K. Istambouli and S. Nelson. Quandle module quivers. *J. Knot Theory Ramifications*, 29(12):2050084, 14, 2020.
- [10] D. Joyce. A classifying invariant of knots, the knot quandle. *J. Pure Appl. Algebra*, 23(1):37–65, 1982.
- [11] L. H. Kauffman. Virtual knot theory. *European J. Combin.*, 20(7):663–690, 1999.
- [12] A. Kazakov. The state-sum invariants for virtual knots.
- [13] S. V. Matveev. Distributive groupoids in knot theory. *Mat. Sb. (N.S.)*, 119(161)(1):78–88, 160, 1982.

DEPARTMENT OF MATHEMATICAL SCIENCES
 CLAREMONT MCKENNA COLLEGE
 850 COLUMBIA AVE.
 CLAREMONT, CA 91711